Available online at www.sciencedirect.com
ScienceDirect
Journal of Sound and Vibration 314 (2008) 657–671
JOURNAL OF SOUND AND VIBRATION
www.elsevier.com/locate/jsvi

# Wave propagation across the boundary between two dissimilar poroelastic solids

M.D. Sharma

*Department of Mathematics, Kurukshetra University, Kurukshetra 136 119, India*

Received 10 August 2007; received in revised form 16 November 2007; accepted 4 January 2008
Handling Editor: L.G. Tham
Available online 14 February 2008

**Abstract**

Two dissimilar isotropic porous media are in welded contact at a plane interface between them. Different sets of boundary conditions are explained to represent the continuity requirements at the common boundary. These are derived from physically grounded principles with mathematical check on the conservation of energy. A new parameter is defined to represent the possible extent of connections between the surface pores of two solids at their common interface. A set of boundary conditions is derived to represent the partial connection of surface pores at the porous–porous interface. Such a partial connection is considered as a basis for an imperfect bonding between two saturated porous solids. At the plane interface, the imperfection in welded bonding is represented by tangential slipping and, hence, results in the dissipation of a part of strain energy.

Three types of waves propagate in an isotropic fluid-saturated porous medium. Incidence of a wave at the interface results in three reflected and three refracted waves. Partition of incident energy among the reflected and refracted waves is studied for incidence of each of the three types of waves. Numerical example calculates the energy shares of reflected and refracted waves at the plane interface between kerosene-saturated sandstone and water-saturated lime-stone. These energy shares are compared for different sets of boundary conditions discussed in the study.


## 1. Introduction

A poroelastic solid is viewed as an elastic matrix with a Newtonian-fluid filling its connected pores. Dynamic behavior of fluid-saturated porous media is attracting wide attention due to their importance in modeling the sedimentary materials encountered in the fields of acoustics, oil exploration, earthquake engineering, soil dynamics and hydrology. The dynamical equations formulated by Biot [1] have been serving as a basis to study wave propagation problems in poroelastic media. Biot [2] extended the acoustic propagation theory in the wider context of the mechanics of porous media. Biot [3] developed the new features of the extended theory, and obtained new and simplified fundamental equations for wave propagation in poroelastic solids. Deresiewicz and Skalak [4] extended the Neumann's uniqueness theorem of elasticity to porous solids and discovered the boundary conditions to represent the continuity requirements at the boundaries of a porous solid. Most of the propagation problems in porous media have been solved using these boundary conditions.

*E-mail address:* mohan_here@rediffmail.com

0022-460X/$ - see front matter © 2008 Elsevier Ltd. All rights reserved.
doi:10.1016/j.jsv.2008.01.023

However, in the intervening period, serious efforts [5–9] have been made to work upon these boundary conditions. Denneman et al. [9] is a recent one that has renewed the attention to the pores, being closed or open. The studies on wave propagation at a boundary between two different porous media are not very large in number. These studies, however, explain various applications of the wave propagation through layered porous media [10–13]. More recently, Vashisth and Khurana [14] studied the wave propagation in stratified porous media using a transfer matrix approach. The porous layers were assumed transversely isotropic with imperfect bonding between them. In all of the studies, the pores of two continuing porous media were assumed to be fully connected. On the other hand, Sharma and Saini [15] discussed the effect of partial connections between the surface pores of two porous solids on the reflection and refraction at their interface. Pore alignment of two porous media were related to the difference in the pressures of the pore-fluids at the interface.

Most of the studies on wave propagation in porous media prefer to use the elastodynamics of Biot's theories and the boundary conditions of Deresiewicz and Skalak [4], for example, Pride et al. [16], Kaynia and Banerjee [17], Chen [18], Gurevich and Schoenberg [8], Denneman et al. [9], Sharma [19–21]. For propagation in stratified media, the assumption that the surface pores of two dissimilar porous media are fully connected at the interface appears to be a too ideal situation. Hence, the boundary conditions from Deresiewicz and Skalak [4], representing such an ideal situation, may not be able to provide a true practical solution, particularly, for simulation studies. A more appropriate solution for such studies may be achieved through a set of more appropriate boundary conditions. Researchers in the field may agree that attention is very much due to these four-decades old boundary conditions.

The work presented suggests and discusses the different sets of boundary conditions to represent the connection between pores at the welded interface. A case of loose contact at the interface is also considered when the surface pores of two media are not fully connected. A numerical example is computed to observe the effects of the different sets of boundary conditions on the energy partition among the waves, reflected and refracted at the porous–porous interface. This study is an effort to provide options in selecting the boundary conditions for interpretation of real data on wave propagation in porous-layered materials.

## 2. Wave propagation in poroelastic solids

Following Biot [2,3], a set of differential equations governs the particle motion in an isotropic porous solid frame saturated by a non-viscous fluid. These equations, in the absence of body forces, are given by

$$\begin{aligned} \tau_{ij,j} &= \rho\ddot{u}_i + \rho_f\ddot{w}_i, \\ (-p_f)_{,i} &= \rho_f\ddot{u}_i + q\ddot{w}_i, \end{aligned} \tag{1}$$

where $\tau_{ij}$ and $p_f$ are the stress components in porous aggregate and fluid pressure, respectively. The $u_i$ are the components of the displacements for the solid and $w_i$ are the components of average displacement of fluid relative to the solid. Indices can take the values 1, 2 and 3. Summation convention is valid for repeated indices. The comma (,) before an index represents partial space differentiation and dot over a variable represents partial time derivative. The $\rho$ and $\rho_f$ are the densities of porous aggregate and pore-fluid, respectively. The inertial parameter $q$ controls dynamical coupling between fluid and solid phases.

The stresses in the isotropic solid matrix of porous aggregate, following Biot [2], are defined as

$$\sigma_{ij} = (\lambda u_{k,k})\delta_{ij} + \mu(u_{i,j} + u_{j,i}), \tag{2}$$

and these are related to $\tau_{ij}$ by

$$\tau_{ij} = \sigma_{ij} + \alpha(-p_f)\delta_{ij}, \tag{3}$$

through the parameter $\alpha$ to represent the elastic coupling between the two constituents. $\delta_{ij}$ is Kronecker delta. Finally, using the above relations, the stresses in the porous aggregate and pore-fluid, are expressed as

$$\begin{aligned} \tau_{ij} &= [(\lambda + \alpha^2 M)u_{k,k} + \alpha M w_{k,k}]\delta_{ij} + \mu(u_{i,j} + u_{j,i}), \\ -p_f &= M(\alpha u_{k,k} + w_{k,k}), \end{aligned} \tag{4}$$

where $\lambda$, $\mu$, $M$ are the elastic constants.

To seek the harmonic solution of Eq. (1), for the propagation of plane waves, write

$$u_i = S_i \exp\{\mathrm{i}\omega(p_k x_k - t)\},$$
$$w_i = F_i \exp\{\mathrm{i}\omega(p_k x_k - t)\} \quad (i = 1, 2, 3), \tag{5}$$

where $\omega$ is angular frequency and components $(p_1, p_2, p_3)$ define slowness vector $\mathbf{p}$. In terms of phase velocity $V$, the slowness vector $\mathbf{p} = \mathbf{N}/V$, where the normalized slowness vector $\mathbf{N} = (n_1, n_2, n_3)$ represents the direction of phase propagation. The vectors $(S_1, S_2, S_3)$ and $(F_1, F_2, F_3)$ define the polarizations for the motions of the solid and fluid particles in the porous medium. Substituting Eq. (5) in Eq. (1) yields a system of six equations, given by

$$\{(\lambda + \mu + \alpha^2 M)n_i n_k + (\mu - \rho V^2)\delta_{ik}\}S_k = (\rho_f V^2 \delta_{ik} - \alpha M n_i n_k)F_k,$$
$$(\rho_f V^2 \delta_{ik} - \alpha M n_i n_k)S_k = (M n_i n_k - q V^2 \delta_{ik})F_k. \tag{6}$$

This system is solved into a relation

$$F_i = \Gamma_{ij} S_j; \quad \boldsymbol{\Gamma} = \frac{\rho_f}{q}(-\mathbf{I} + \mathbf{N}^{\mathrm{T}}\mathbf{N}) - \frac{\rho_f V^2 - \alpha M}{qV^2 - M}\mathbf{N}^{\mathrm{T}}\mathbf{N}, \tag{7}$$

and a subsystem, given by

$$W_{ik} S_k = 0, \quad W = g\mathbf{N}^{\mathrm{T}}\mathbf{N} + h(\mathbf{I} - \mathbf{N}^{\mathrm{T}}\mathbf{N});$$
$$g = (\lambda + 2\mu + \alpha^2 M - \rho V^2) + \frac{(\rho_f V^2 - \alpha M)^2}{qV^2 - M}, \quad h = \mu - \left(\rho - \frac{\rho_f^2}{q}\right)V^2, \tag{8}$$

where $\mathbf{I}$ is a third-order identity matrix and $\mathbf{N}^{\mathrm{T}}$ denotes the transpose of row matrix $\mathbf{N}$. The expression (7) relates the displacements ($\mathbf{u}$ and $\mathbf{w}$) of two constituents phases in the porous aggregate. The set of Eqs. (8) explains the propagation phenomenon in the medium. This latter set may be termed as modified Kelvin–Christoffel equation [22] for wave propagation in isotropic fluid-saturated porous media. Existence of non-trivial solution of these equations is ensured by

$$(\rho q - \rho_f^2)V^4 - [q(\lambda + 2\mu + \alpha^2 M) + \rho M - 2\rho_f \alpha M]V^2 + (\lambda + 2\mu)M = 0, \tag{9}$$

$$(\rho q - \rho_f^2)V^2 - \mu q = 0. \tag{10}$$

The roots of quadratic equation (9) define the phase velocities of two longitudinal waves in the porous medium. The second equation gives the velocity of lone transverse waves in the medium. On replacing $q$ with $q + \mathrm{i}(\eta/\omega\chi)$, Eqs. (9) and (10) explain the wave propagation in porous media, in the presence of dissipation represented by pore-fluid viscosity $\eta$ and pore permeability $\chi$. For high frequency, $\eta$ is multiplied with a correction factor.

Polarization vector $(S_1, S_2, S_3)$, corresponding to Eq. (9), is calculated to be parallel to $\mathbf{N}$ and hence the two waves with velocities (say, $V_1$ and $V_2$ ) defined by this equation are longitudinal waves. $V_1$ is assumed to be greater than $V_2$. This identifies $V_1$ and $V_2$ as the velocities of *fast P* (or $P_f$) and *slow P* (or $P_s$) waves, respectively. From Eq. (7), the polarizations of the fluid particles, for two longitudinal waves, are given by the relation

$$(F_1, F_2, F_3) = -\left(\frac{\rho_f V^2 - \alpha M}{qV^2 - M}\right)(S_1, S_2, S_3), \quad V = V_1,\ V_2. \tag{11}$$

Similarly, Eqs. (8) and (10) yield polarization vector $(S_1, S_2, S_3)$, for the lone transverse wave. This is represented through a row/column of the singular matrix $(\mathbf{I} - \mathbf{N}^{\mathrm{T}}\mathbf{N})$. Such a transverse wave propagates with velocity, say $V_3$, given by $V_3^2 = \mu/(\rho - \rho_f^2/q)$. Corresponding to these waves, the polarization vector $(F_1, F_2, F_3)$ for the fluid particles is calculated from the relation

$$(F_1, F_2, F_3) = -\left(\frac{\rho_f}{q}\right)(S_1, S_2, S_3). \tag{12}$$

Eqs. (9) and (10) are same as those obtained in Biot's theory. But, the significance of the procedure explained above lies in its different manner which is used, generally, to study three-dimensional wave propagation in anisotropic media. So the same procedure can yield the corresponding expressions for wave propagation in anisotropic media and these expressions can be compared/checked at different steps with those derived in this section.

## 3. Formulation of the problem

Consider two dissimilar saturated non-dissipative isotropic porous solids having a common boundary. In the Cartesian coordinate system $(x, y, z)$, let the plane $z = 0$ define this common boundary which is separating the two dissimilar porous media (say, $M_1$ and $M_2$). A wave travels through the medium $M_1$ (i.e., $z>0$) with velocity $V_o$ and incident at the interface making an angle $\theta_o$ to the $z$-axis pointing into this medium. For two-dimensional motion in the $x$–$z$ plane, unit vector $(\sin\theta_o, 0, \cos\theta_o)$ represents phase direction of the incident wave. The incident angle may vary from 0 to $\pi/2$. Such an incidence results in three waves reflected back into the medium $M_1$ and three waves refracted to the continuing medium $M_2$. The primed ($'$) quantities separate the medium $M_2$ from $M_1$. The row vectors $(n_1^{(k)}, n_2^{(k)}, n_3^{(k)})$, $(k = 1, 2, 3)$, denote the phase directions of three reflected waves in porous medium.

The displacements in the porous medium $M_1$ are expressed as

$$\begin{aligned} u_j &= S_j \exp\left\{ i\omega\left(\frac{1}{V_o} n_k x_k - t\right)\right\} + \sum_{l=1}^{3} f_l S_j^{(l)} \exp\left\{ i\omega\left(\frac{1}{V_l} n_k^{(l)} x_k - t\right)\right\}; \\ w_j &= F_j \exp\left\{ i\omega\left(\frac{1}{V_o} n_k x_k - t\right)\right\} + \sum_{l=1}^{3} f_l F_j^{(l)} \exp\left\{ i\omega\left(\frac{1}{V_l} n_k^{(l)} x_k - t\right)\right\} \quad (j = x, y, z), \end{aligned} \tag{13}$$

where the values 1–3 of index $l$ represent the $P_f, P_s, S$ waves, respectively. The $f_l$ are relative excitation factors for the three reflected waves. We have $n_j^{(l)} n_j^{(l)} = 1$, and from Snell's law, $n_1^{(l)}/v_l = \sin\theta_o/V_o,\ n_2^{(l)} = 0$.

Similarly, for the waves refracted to medium $M_2$, the displacements are expressed as

$$\begin{aligned} u'_j &= \sum_{l=1}^{3} f'_l S_j^{\prime(l)} \exp\left\{ i\omega\left(\frac{1}{V'_l} m_k^{(l)} x_k - t\right)\right\}; \\ w'_j &= \sum_{l=1}^{3} f'_l F_j^{\prime(l)} \exp\left\{ i\omega\left(\frac{1}{V'_l} m_k^{(l)} x_k - t\right)\right\} \quad (j = x, y, z). \end{aligned} \tag{14}$$

The $f'_l$ are relative excitation factors for the refracted waves. We have $m_j^{(l)} m_j^{(l)} = 1$, and from Snell's law, $m_1^{(l)}/V_l = \sin\theta_o/V_o,\ m_2^{(l)} = 0$.

## 4. Boundary conditions

The boundary conditions at a boundary of porous solid come from the physical situations existing there. The energy consideration for the medium and the continuity equation for fluid-flow are the fundamental requirements. The energy in a poroelastic body is calculated from the stresses and particle velocities of fluid and solid particles. In the present geometry of porous–porous contact, energy balance is maintained through the equation

$$\tau_{zz}\dot{u}_z + \tau_{zx}\dot{u}_x - p_f\dot{w}_z = \tau'_{zz}\dot{u}'_z + \tau'_{zx}\dot{u}'_x - p'_f\dot{w}'_z. \tag{15}$$

### 4.1. Welded-contact interface

Let us start with the simplest case of welded contact interface such that the surface pores of the two media are fully connected. Following Deresiewicz and Skalak [4], the appropriate boundary conditions to be satisfied at the interface $z = 0$, are

$$\begin{aligned} &\text{(i) } \tau_{zz} = \tau'_{zz}; \quad \text{(ii) } \dot{u}_z = \dot{u}'_z; \quad \text{(iii) } \tau_{zx} = \tau'_{zx}; \\ &\text{(iv) } \dot{u}_x = \dot{u}'_x; \quad \text{(v) } p_f = p'_f; \quad \text{(vi) } \dot{w}_z = \dot{w}'_z. \end{aligned} \tag{16}$$

The boundary conditions (i) and (iii) represent the continuities of normal and tangential stresses between the two media. Similarly, the conditions (ii) and (iv) ensure the continuities of normal and tangential components of displacements of solid particles in two porous media. The relation (v) is the continuity of pressures of the pore-fluids filling the pores on either side of the interface $z=0$. These conditions ensure the conservation of energy at the interface. The boundary condition (vi) does not seem to be satisfying the equation of continuity for pore-fluids. This is actually a continuity of averaged velocities of the fluids discharged out of the surface pores. This becomes the continuity equation if $\rho_f=\rho'_f$, for example, same pore-fluid in the pores on either side of interface. As an alternative, the boundary conditions (v) and (vi) may change to

$$\text{(v) } p'_f/\rho'_f=p_f/\rho_f; \quad \text{(vi) } \rho_f\dot{w}_z=\rho'_f\dot{w}'_z. \tag{17}$$

Now, the condition (vi) in Eq. (17) ensures the continuity of mass (not velocity) of the fluid discharged out of the pores at the interface and hence is the equation of continuity for the interstitial fluids. The boundary condition (v) in Eq. (17) does not ensure the continuity of fluid pressures at the interface between two media (except, when both the pore-fluids have the same density) and hence allows the fluid-flow (inside the fully connected pores) across the interface. An aspect of allowing the fluid-flow across the interface is that the high-pressure fluid is pushing the low-pressure fluid, for example, oil–water fluid substitution events in reservoirs [23]. Such a substitution is considered in the horizontal flow of fluids in the reservoir rocks around a producing well. In that case, the same velocity of fluid particles on either side of (vertical) interface may not allow the mixing of fluid. Then, due to the same potential energy (per unit mass) in both media, the boundary condition (v) in Eq. (17) becomes the Bernoulli's equation ensuring the conservation of energy at the interface. On the other hand, to avoid the mixing of two pore fluids at the interface, the two conditions (v) and (vi) in Eq. (16) are changed to

$$\text{(v) } f'p'_f=fp_f; \quad \text{(vi) } \dot{U}_z=\dot{U}'_z, \tag{18}$$

where $\dot{U}_z$ defines the normal velocity of fluid particles in $\dot{w}_z=f(\dot{u}_z-\dot{U}_z)$. The condition (v) represents the continuity of averaged fluid pressures at the interface and the conservation of energy is not disturbed with these conditions.

Fully connected pores at the interface, as used by Deresiewicz and Skalak [4], may not be a realistic situation. For example, the surface pores at the common (plane) boundary of two porous media may not connect fully, even when they have same porosity. Hence, a new parameter is required to represent the effective connections between the surface-pores of two media at the interface. Let this parameter, $\phi$, be defined as

$$\phi=\frac{\min(f,f')}{\max(f,f')}v, \tag{19}$$

where $f$ and $f'$ are porosities of the two porous media. The value of $\phi$ lies between 0 and 1. The value of $\phi$ can be zero when, either $v=0$ or one of the porosities is zero. That means no connection between pores at the interface. The value 1 of $\phi$ means fully connected pores and can be achieved only when $f=f'$ and $v=1$. So, $v$ acts as a likelihood parameter that may be defined as the probability that the surface pores of two porous solids of same porosity are fully connected. Moreover, instead of pore pressure, the fluid discharge out of the pores should depend upon the differential pressure (difference between normal stress in porous matrix and fluid pressure) existing in the porous aggregate. In terms of differential stress components the energy balance equation (15) is rewritten as

$$\tau_{zz}(\dot{u}_z+\dot{w}_z)+\tau_{zx}\dot{u}_x-(p_f+\tau_{zz})\dot{w}_z=\tau'_{zz}(\dot{u}'_z+\dot{w}'_z)+\tau'_{zx}\dot{u}'_x-(p'_f+\tau'_{zz})\dot{w}'_z. \tag{20}$$

The boundary conditions are defined as

$$\text{(i) } \tau_{zz}=\tau'_{zz}; \quad \text{(ii) } \dot{u}_z+\dot{w}_z=\dot{u}'_z+\dot{w}'_z; \quad \text{(iii) } \tau_{zx}=\tau'_{zx}; \quad \text{(iv) } \dot{u}_x=\dot{u}'_x;$$

$$\text{(v) } \phi(p_f+\tau_{zz})=Z(1-\phi)\dot{w}'_z; \quad \text{(vi) } \phi(p'_f+\tau'_{zz})=Z(1-\phi)\dot{w}_z, \tag{21}$$

where $Z$ (a constant) is assumed to be a non-zero, finite value for surface flow impedance [9], when the pores are partially connected (i.e., $0<\phi<1$). These boundary conditions do not disturb the conservation of energy

at the interface. These conditions involve two parameters $Z$ and $\phi$, but, in fact, a single unknown (i.e., $Z(1-\phi)/\phi$) is relating the differential stress and fluid discharge on either side of the interface.

For an ideal but non-realistic situation given by $\phi = 1$, the above boundary conditions reduce to

$$\text{(v) } p_f + \tau_{zz} = 0; \quad \text{(vi) } p'_f + \tau'_{zz} = 0. \tag{22}$$

This provides an alternative to the boundary conditions (v) and (vi) in Eq. (16) for fully connected pores. For a theoretical case of no connection between the surface pores of two media, the value $\phi = 0$ changes these two boundary conditions to

$$\text{(v) } \dot{w}_z = 0; \quad \text{(vi) } \dot{w}'_z = 0, \tag{23}$$

which are same as obtained in Ref. [4].

### 4.2. Loose contact interface

When the surface pores are not fully connected then, at the interface, pore-fluid of one medium will be in contact with the solid surface of the other medium. In aggregate, such a contact will be weaker than the welded contact, generally assumed, between two solids. This may be termed as loose contact and is represented by the presence of a thin layer of fluid at the common surface between two porous media. For loose bonding between the two media, following Vashisth et al. [24], the boundary condition (iv) changes to

$$\text{(iv) } \psi\tau_{zx} = (1-\psi)T(\dot{u}_x - \dot{u}'_x), \tag{24}$$

where, the parameter $\psi$, in $(0, 1)$, represents the loose bonding from smooth contact ($\psi = 0$) to welded contact ($\psi = 1$). The impedance $T$ is a non-zero finite positive value and represent the resistance to the free discharge of pore-fluid at the interface. The tangential stress at the interface is proportional to the tangential slip allowed at the interface due to loose bonding. Such a frictional slip should dissipate a part of energy at the interface. Hence, in deviation from the welded contact, at the loosely bonded interface ($0<\psi<1$) represented by condition (24), the energy conservation is achieved with its dissipated part. In this case, the sum of the energies of reflected and refracted waves at the interface will be smaller than the incident energy.

## 5. Reflection and refraction coefficients

Distribution of energy among the reflected and refracted waves is considered across a surface element of unit area at the plane $z = 0$. The scalar product of surface traction and particle velocity per unit area, denoted by $P^*$, represents the rate at which the energy is communicated per unit area of the surface. The time average of $P^*$ over a period, denoted by $\langle P^* \rangle$, represents the average intensity of energy transmission. On the surface with normal along $z$-direction, the average energy intensities of the waves in a porous medium are defined by

$$\langle P^*_{jk} \rangle = 0.5\mathrm{Re}[\tau^{(j)}_{zz}\,\mathrm{conj}(\dot{u}^{(k)}_z) + \tau^{(j)}_{zx}\,\mathrm{conj}(\dot{u}^{(k)}_x) + (-p^{(j)}_f)\,\mathrm{conj}(\dot{w}^{(k)}_z)] \quad (j,k = 1,2,3). \tag{25}$$

With $\langle P^*_I \rangle$ defining the energy intensity of the incident wave, an energy matrix $E_{jk} = \langle P^*_{jk} \rangle / \langle P^*_I \rangle$ $(j,k = 1,2,3)$, calculates the distribution of energy among the three waves traveling into the poroelastic medium. Sum of all the off-diagonal entries of this energy matrix gives the share of interaction energy among the different waves in the medium. In case of non-dissipative isotropic medium, these entries form a skew-symmetric matrix and the resultant interaction energy vanishes. The magnitude of the diagonal entries of $\mathbf{E}$, however, represent the energy shares of the three reflected waves in the medium. Let $E_{11}, E_{22}, E_{33}$ be termed as the reflection coefficients for $P_f, P_s, S$ waves, respectively. Similarly, another matrix $E'_{jk}$ calculates the energy ratios (termed as refraction coefficients) of the waves refracted to the continuing medium. A relation, given by $E'_{11} + E'_{22} + E'_{33} + E_{11} + E_{22} + E_{33} = 1$, ensures the conservation of energy across the interface.

The displacements defined in Eqs. (13) and (14) are used in the boundary conditions at the interface between two porous solids. The six boundary conditions, defined in previous section, are satisfied through a system of six linear inhomogeneous equations inn $f_1, f_2, f_3$ and $f'_1, f'_2, f'_3$. This system is solved numerically through Gauss elimination method. Solution is, then, used to calculate the energy ratios $E_{ij}$ and $E'_{ij}$ and, hence, to check the conservation of energy.

## 6. Numerical example

Purpose of the numerical example is to check the impact of suggested boundary conditions on the propagation of three waves across the interface between two dissimilar poroelastic solids. The medium chosen for the numerical example is the kerosene-saturated sandstone in contact with water-saturated limestone. Following Yew and Jogi [25], the values of relevant coefficients for the two porous solids are as follows:

(i) *for kerosene-saturated sandstone* (*medium* $M_1$):

$$\lambda = 2.771\,\text{GPa}, \quad \mu = 2.765\,\text{GPa}, \quad M = 4.873\,\text{GPa}, \quad \alpha = 0.85,$$
$$\rho = 2137\,\text{kg/m}^3, \quad \rho_f = 820\,\text{kg/m}^3, \quad q = 3316\,\text{kg/m}^3, \quad f = 0.26.$$

(ii) *for water-saturated limestone* (*medium* $M_2$):

$$\lambda' = 1.444\,\text{GPa}, \quad \mu' = 12.09\,\text{GPa}, \quad M' = 15.91\,\text{GPa}, \quad \alpha' = 0.262,$$
$$\rho = 2240\,\text{kg/m}^3, \quad \rho_f' = 1000\,\text{kg/m}^3, \quad q' = 6944\,\text{kg/m}^3, \quad f' = 0.144.$$

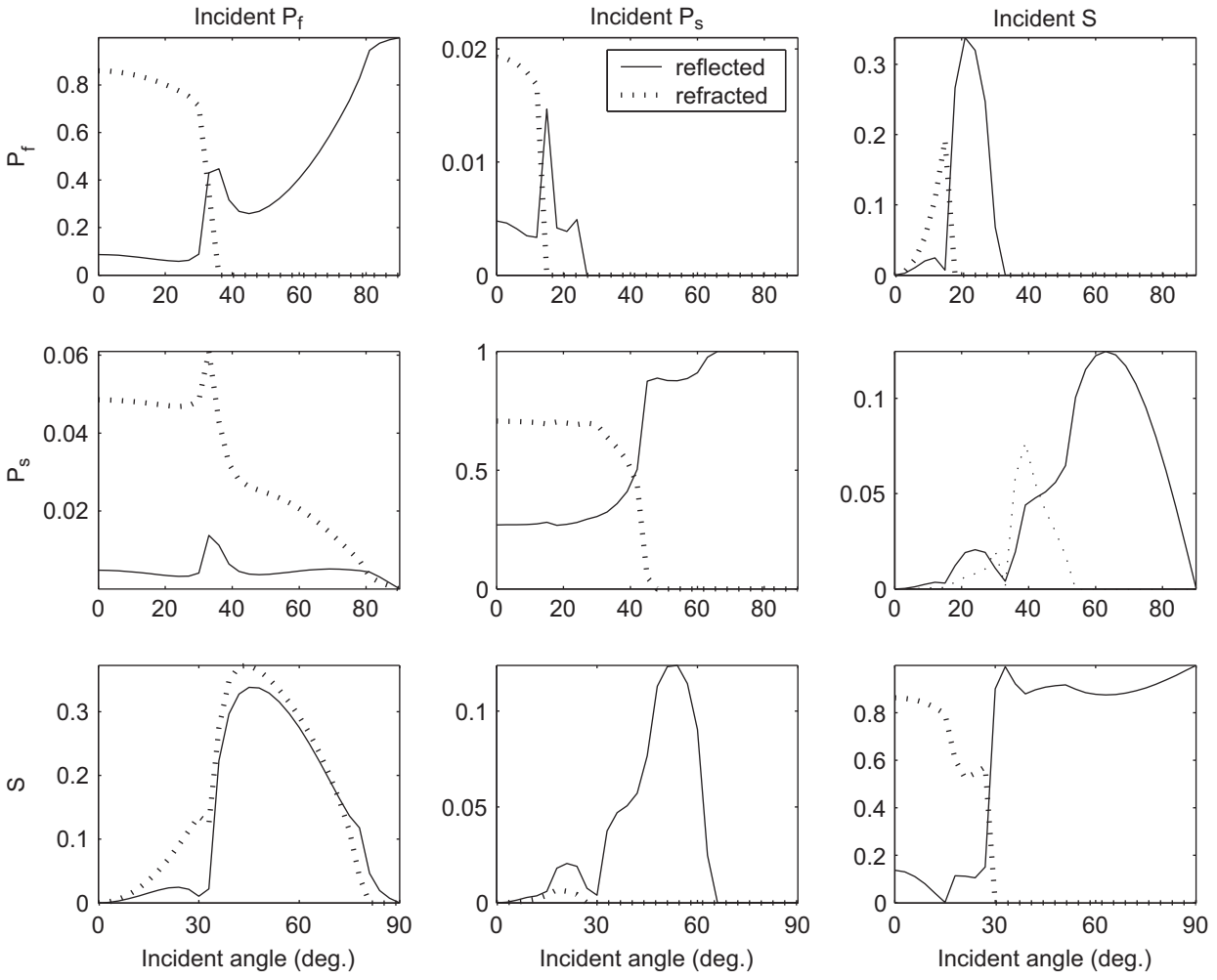


Fig. 1. Energy share of reflected and refracted waves for fully connected pores at welded interface between kerosene-saturated sandstone and water-saturated limestone.

These numerical values are used to calculate the reflection and refraction coefficients of $P_f, P_s$ and $S$ waves. Incidence of each of the three $(P_f, P_s, S)$ waves is considered with angle of incidence varying from 0 to $\pi/2$. Variations of these coefficients with the incident direction are plotted in Figs. 1–7. Details are as follows.

For the welded interface with fully connected surface pores, as defined by boundary conditions (16), variations of reflection and refraction coefficients are plotted in Fig. 1. The corresponding coefficients for the alternate boundary conditions, as defined in Eq. (17), are shown in Fig. 2. The no-mixing of pore fluids are represented by conditions (18) and the corresponding energy partition in this case is as shown in Fig. 3. For a fixed value of impedance constant $Z = 2\,\text{MPa s/m}$, the energy shares of reflected and refracted waves at the interface with partial pore-connections (i.e., $v = 0.1, 0.5, 1$), are shown in Fig. 4. Effect of a change in the value of impedance constant (i.e., $Z = 0.1,\ 2,\ 5\,\text{MPa s/m}$) on energy partition is exhibited in Fig. 5, for the pore-connections defined by $v = 0.5$.

Fig. 6 presents energy partition at the loosely bonded interface ($\psi = 0.3, 0.6, 0.9$) between two porous solids when their surface-pores are partially connected ($v = 0.9$). The surface flow impedance is fixed with $Z = T = 1\,\text{MPa s/m}$. For the case of imperfect (or loose) bonding between two solids, the sum of energy shares of reflected and refracted waves is less than one. This implies that a part of the incident energy is dissipated at the interface. The dissipated energy changes with the values of impedance $T$ and bonding

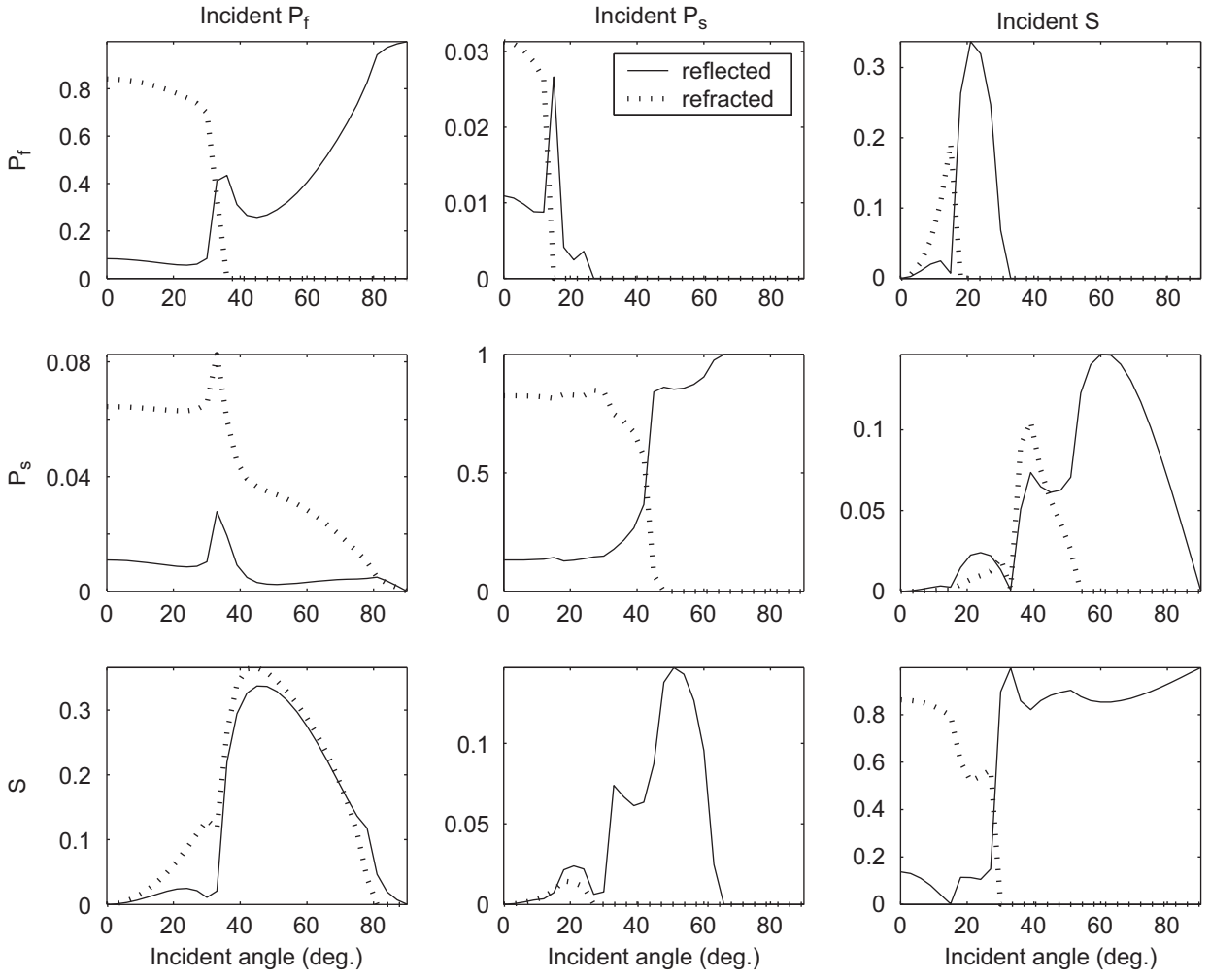


Fig. 2. Same as Fig. 1, but with alternate boundary conditions allowing fluid flow in pores across the interface.

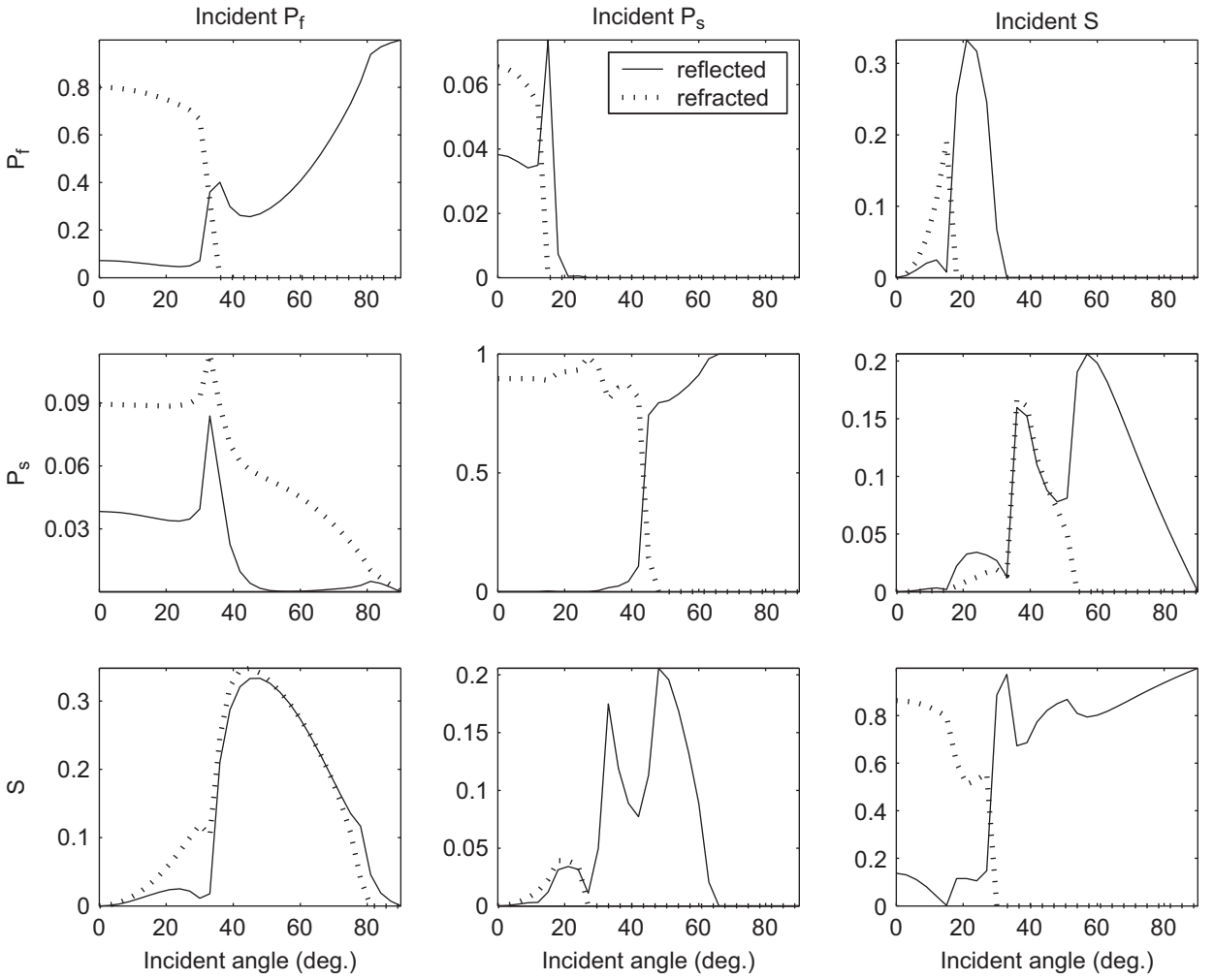


Fig. 3. Same as Fig. 1, but with boundary conditions to avoid mixing of pore-fluids in fully connected pores.

parameter $\psi$. Fig. 7. shows the variations of this energy with incident direction for $T = 0.1, 1, 10$ MPa s/m and $\psi = 0.1, 0.5, 0.9$.

## 7. Discussion of numerical results

Fig. 1 shows the variations in energy partition with the angle of incidence when the surface pores are fully connected at the welded interface between two porous media. The boundary conditions of Deresiewicz and Skalak [4], given by Eq. (16), are used. For incident $P_f$ waves, the energy is shared mainly among $P_f$ and $S$ waves. Refracted $P_s$ waves are stronger than the reflected $P_s$ waves. Similarly, for the incidence of $P_s$ waves, the reflected and refracted $P_f$ waves are very weak. Reflected $P_s$ waves from incident $S$ waves are much stronger when compared to those from incident $P_f$ wave.

The energy partition in Fig. 2 is also at the welded interface with fully connected pores, but with alternate boundary conditions (17). These boundary conditions ensure the equation of continuity for the fluid-flow (in pores) across the interface. The reflected and refracted $P_s$ waves, from incident $P_f$ wave, are much stronger than in Fig. 1. These $P_s$ waves get the additional energies from refracted $P_f$ wave. The energies of reflected and refracted $S$ waves are the least affected with the change in boundary conditions. For incident $P_s$ wave,

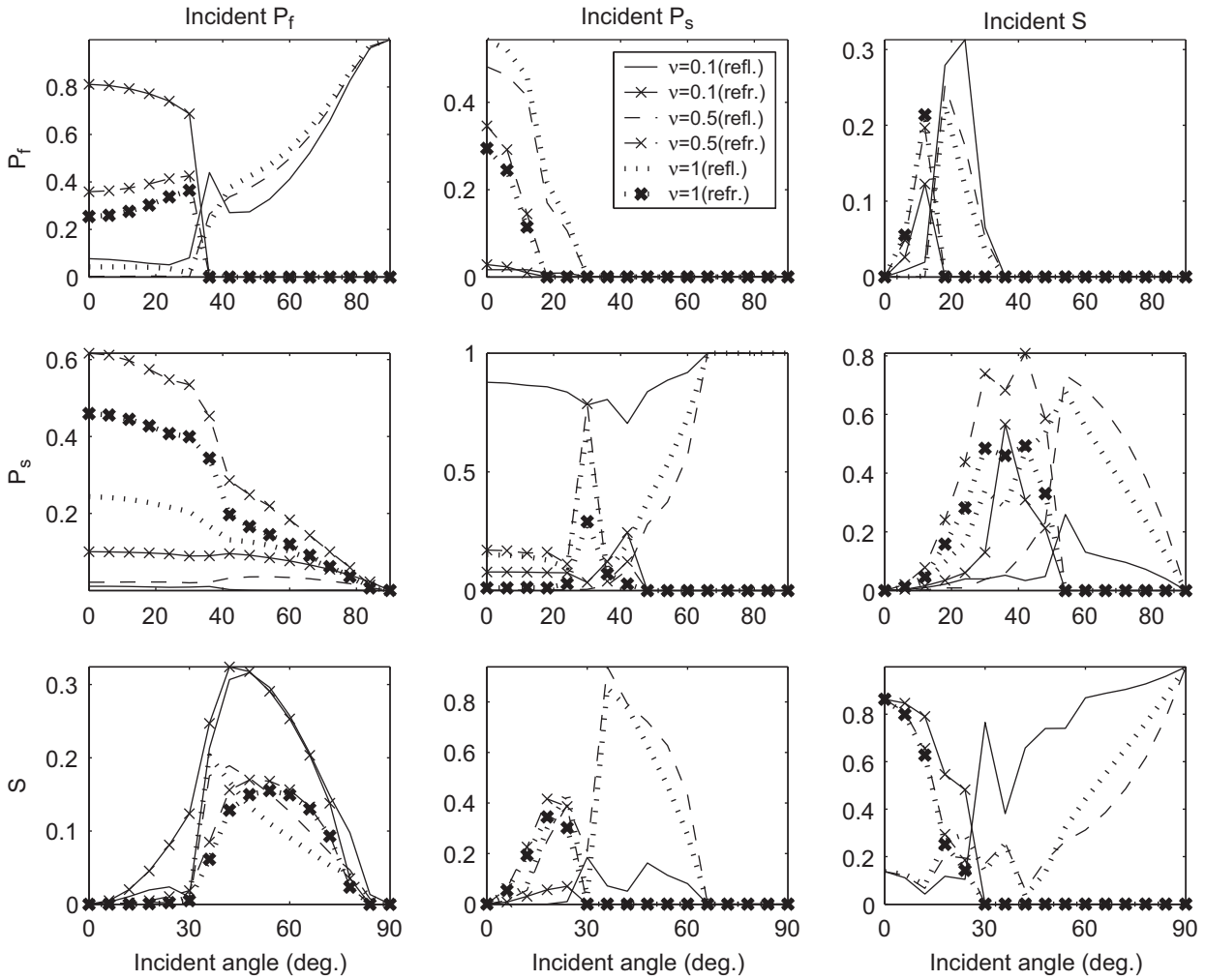


Fig. 4. Energy partition at welded interface between kerosene-saturated sandstone and water-saturated limestone, for partially connected pores; fixed impedance $Z = 2\,\mathrm{MPa\,s/m}$.

reflected/refracted $P_f$ and refracted $P_s$ waves get stronger at the cost of reflected $P_s$ wave. The reflected and refracted $S$ waves are almost unaffected. These alternative boundary conditions do not show much effect on the reflection/refraction response of incident $S$ wave. The little effect is observed only on the variations of reflected $P_s$ and $S$ energies with incident direction. In general, the comparison of respective plots in Figs. 1 and 2 explain the effects of changes made in boundary conditions to ensure the equation of continuity for pore-fluids across the interface.

Fig. 3 exhibits the energy partition corresponding to the boundary conditions assuming the non-mixing of two pore-fluids at their interface in connecting pores. In comparison to Fig. 2, for incident $P_f$ wave, the reflected/refracted $P_s$ waves gain energy out of the shares of $P_f$ and $S$ waves. For incident $P_s$ wave, the reflected/refracted energies of $P_f$ and $S$ waves may be doubled for some incident directions. Near normal incidence, refracted $P_s$ wave gains energy and even achieve total refraction when the incidence angle is about 25°. Such a total refraction is not observed in Fig. 1 or 2. At the incidence of $S$ wave, beyond the critical angles of $P_f$ waves, the energies of reflected/refracted $P_s$ waves are nearly double to that observed in Fig. 2. These gains in $P_s$ energies are coming from the share of reflected $S$ waves.

Fig. 4 shows the energy partition when the surface pores at the porous–porous interface are genuinely connected. The effects on the energy shares are observed for the different values of likelihood parameter $v$. The

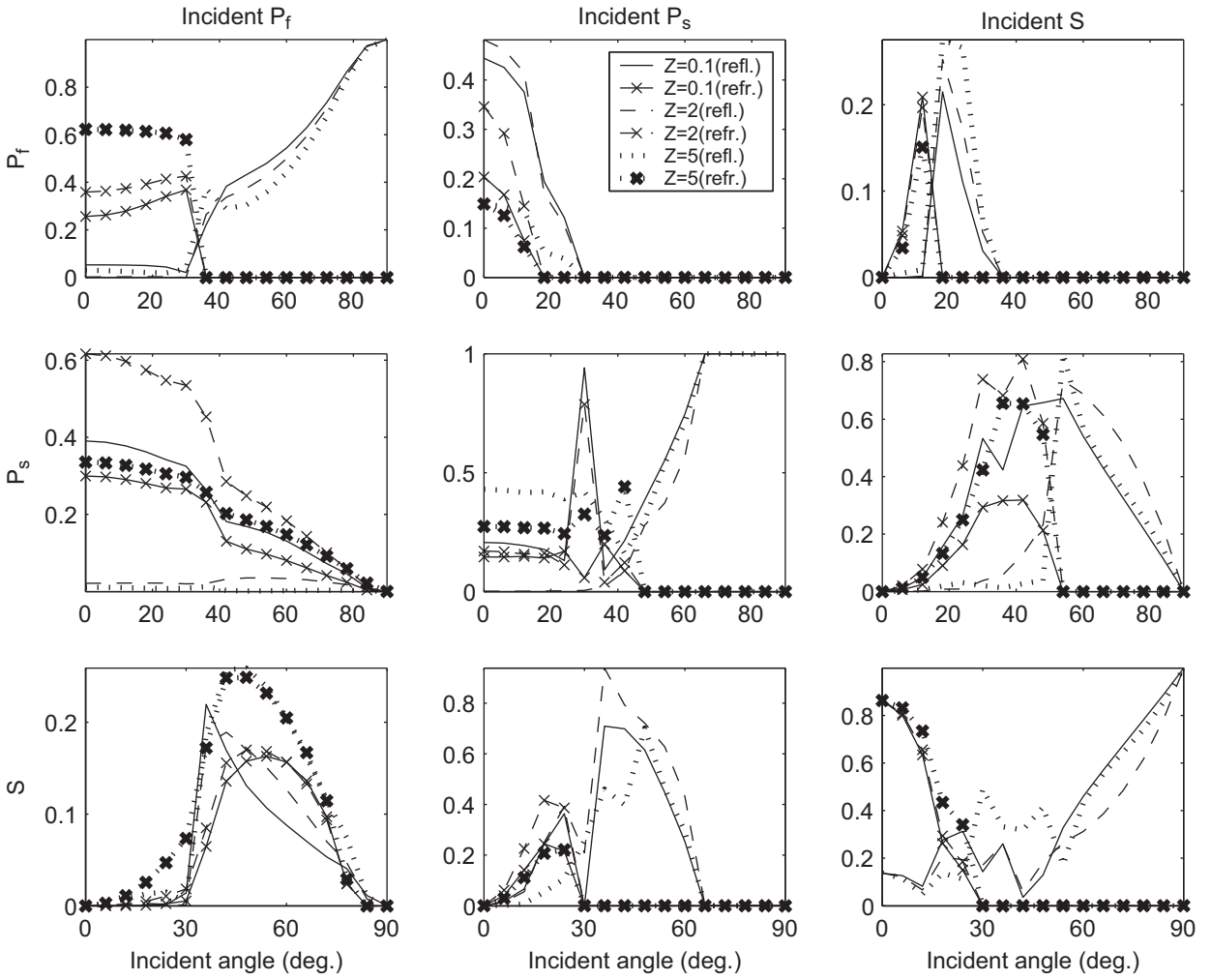


Fig. 5. Same as Fig. 4, but for different impedances (in MPa s/m) and fixed $v = 0.5$.

major effect of the partial pore-connection is the gain in energy share of $P_s$ waves, when the incident waves are $P_f$ or $S$ waves. This gain is more significant when less pores are connected (i.e., $v$ is small). For incidence of $P_f$ waves after the critical angle for refracted $P_f$ waves, increase of $v$ weakens the refracted $P_f$ waves but strengthens the reflected $P_f$ waves. The refracted $P_s$ waves are the strongest for the intermediate value of $v$ whereas the reflected $P_s$ waves get stronger with the increase of $v$. The increase of $v$, however, weakens both reflected and refracted $S$ waves resulting from the incident $P_f$ waves. For incident $P_s$ waves, large changes in energy shares are observed with the change in the connections between surface pores at the interface. However, the effects of this change are nearly opposite on reflected and refracted waves. For incident $S$ waves, the $P_f$ waves appear to be less affected with the change in $v$, while other two waves are affected significantly. Near grazing or normal incidence of $S$ waves, pore-connection level seems to have no effect on energy partition.

Fig. 5 displays the effect of surface flow impedance ($Z$) on the energy shares of reflected and refracted waves. An increase of surface flow impedance shows a significant effect on the energy shares of all the reflected and refracted waves, but for the larger values of $Z$. For example, it is calculated that for values of $Z$, sufficiently less than 1 MPa s/m, the change in $Z$ has negligible effect on the energy partition. The effect of $Z$ is matters more for its value increasing away from 1 MPa s/m. It is also noted that a change in impedance has no effect

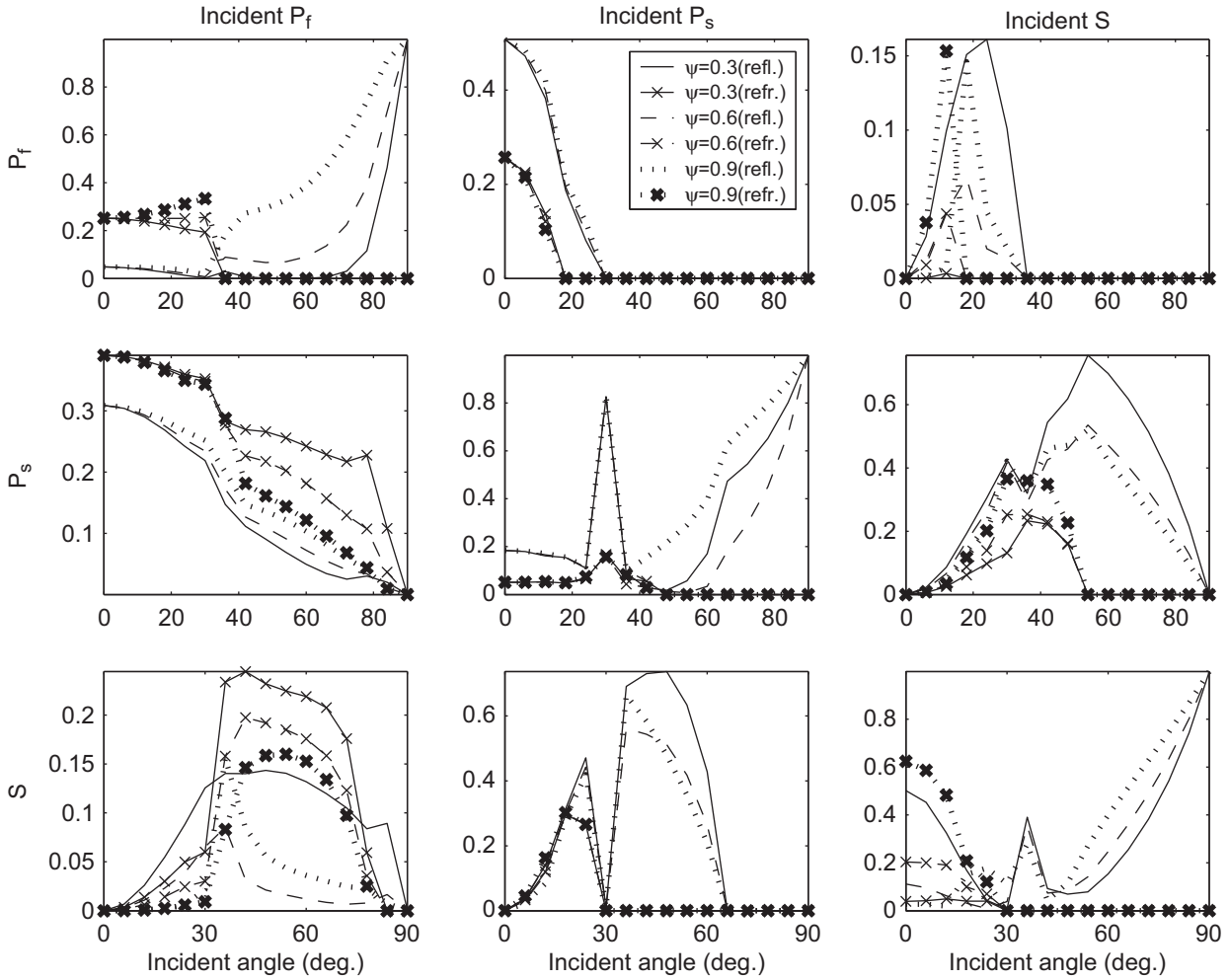


Fig. 6. Energy partition at loosely bonded interface between kerosene-saturated sandstone and water-saturated limestone; fixed $v = 0.5$; fixed impedance $Z = T = 1$ MPa s/m.

near grazing incidence of any of the three waves. For the normal incidence of any of the P waves, the impedance shows its effect on the reflected and refracted P waves only.

Fig. 6 exhibits the effect of loose bonding on energy partition but for pore-connections defined by $v = 0.9$. For incidence of $P_f$ waves beyond the critical angle for refracted $P_f$ waves, the reflected $P_f$ waves get stronger with the increase in bonding parameter $\psi$. In this case, the reflected and refracted $S$ waves are the strongest for the smaller values of $\psi$. The reflected (refracted) $P_s$ waves strengthen (weaken) with the increase of $\psi$. For incident $P_s$ waves, the effect of $\psi$ is observed mainly on reflected $P_s$ waves and a little on reflected S waves. Refracted waves are the least affected with the change in bonding status. For incident $S$ waves, the effect of $\psi$ is quite clear on reflected waves. Reflected $S$ ($P$) waves weaken (strengthen) from the decrease of $\psi$ from 1 to 0. Refracted waves, however, strengthen with the increase of $\psi$. From this figure it is clear that the reflected and refracted waves are not sharing the incident energy completely. The part of energy dissipated due to loose bonding is shown in Fig. 7. It is observed that the energy dissipation is minimum (i.e., zero) when the contact is either smooth (i.e., $\psi = 0$) or the contact is either welded (i.e., $\psi = 1$). For the intermediate values of $\psi$, the dissipated energy may amount to be more than half of the incident energy. Is may be noted from Fig. 7 that for a fixed value of $T = 0.1$ MPa s/m, energy dissipation increases with the increase of bonding parameter $\psi$. On the other hand, for $T = 10$ MPa s/m, energy dissipation decreases with the increase of $\psi$.

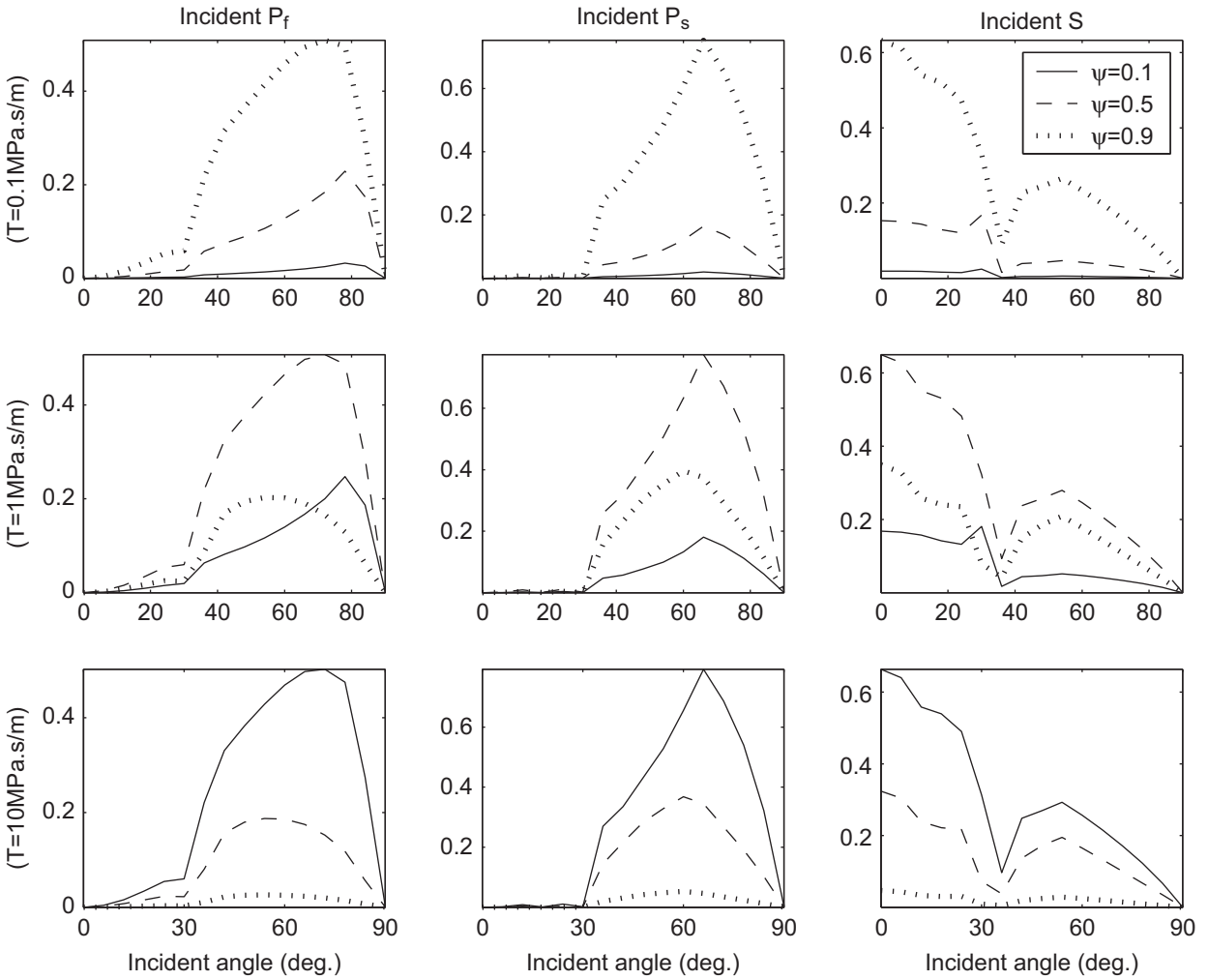


Fig. 7. Variations in the dissipation of energy at the interface with impedance $T$ and bonding parameter $\psi$.

For $T = 1\,\mathrm{MPa\,s/m}$, energy dissipation is maximum when $\psi = 0.5$ and decreases on either side. This may imply that for nearly smooth bonding, the increase of $T$ increases the energy dissipation whereas, for nearly welded bonding, the dissipation decreases with the increase of impedance $T$. For incident P waves, the energy dissipation is minimum for normal as well as grazing incidence. For incident S waves, maximum dissipation is observed for normal incidence and minimum for grazing incidence. A steep rise/fall in energy dissipation is noticed when incident direction comes across a critical angle.

## 8. Concluding remarks

This study considers the different sets of boundary conditions between two dissimilar porous solids and calculates their effect on the energy partition among reflected and refracted waves. The changes in reflection/refraction coefficients are analyzed for a particular numerical model with different values of parameters for pore-connection, loose bonding and impedance. The few conclusions drawn from this analysis may be explained as follows.

(i) Deviation from the equation of continuity for pore-fluid may not have much effect on the energy partition, particularly when the densities of the two fluids filling the pores on either side are nearly same.

Else, such a deviation will become an inherent source of error in the mathematical model of the problem. Moreover, effect of this deviation is observed, mainly, on the strength of $P_s$ wave, which separates the poroelastic propagation from the elastic one.

(ii) The no-mixing restriction on the pore-fluids is also showing its effect on the reflected and refracted $P_s$ waves. This is significant because of the diagnostic importance of the wave in understanding the fluid dynamism in the saturated porous rocks.

(iii) Partial pore-connections have significant effect on the longitudinal waves whereas transverse waves are less affected. Among the longitudinal waves, the refracted $P_s$ wave gains most at the cost of $P_f$ waves.

(iv) Surface flow impedance shows a significant effect on the energy partition but only when its value increases beyond a particular value (e.g., 1 MPa s/m in this study).

(v) Near grazing incidence, the effect of pore-connections and impedance is negligible. $S(P)$ waves are unaffected even at the normal incidence of $P(S)$ waves. For the normal incidence of $S$ waves, the energy partition is unaffected with the changes in pore-connections and impedance.

(vi) Presence of tangential slip at the interface may strengthen the $S$ waves from the incidence of $P$ waves. Similarly, reflected $P$ waves from the incident $S$ waves gain strength when the contact between solids allows slip at the interface.

(vii) The energy dissipation at a loose boundary is smaller for the incident $P_f$ wave as compared to the incidence of $P_s$ and $S$ waves.

This study puts forward some new combinations of boundary conditions at the porous–porous boundary. The suggested combinations represent some realistic physical situations. The energy conservation is kept in mind while translating physical situations into boundary conditions. These boundary conditions may be able to provide more accurate solutions to the problems of dynamics in porous materials. It is very much acceptable that there may be some more combinations of these types that may represent the remaining and possible situations. Author feels that the researchers in the field of structural engineering and exploration may prefer to use the proposed conditions in the simulation studies. The dissipation of a part of energy due to wave-induced slip at the loosely bonded interface certifies the important role of fluid-saturated porous solid layers in sound/shock absorbing packages. The wave propagation procedure explained in Section 2 is presented in a different manner which can be modified with much convenience for a similar study in anisotropic media.

## References

[1] M.A. Biot, The theory of propagation of elastic waves in a fluid-saturated porous solid, I. Low-frequency range, II. Higher frequency range, *Journal of the Acoustical Society of America* 28 (1956) 168–191.

[2] M.A. Biot, Mechanics of deformation and acoustic propagation in porous media, *Journal of Applied Physics* 33 (1962) 1482–1498.

[3] M.A. Biot, Generalized theory of acoustic propagation in porous dissipative media, *Journal of the Acoustical Society of America* 34 (1962) 1254–1264.

[4] H. Deresiewicz, R. Skalak, On uniqueness in dynamic poroelasticity, *Bulletin of the Seismological Society of America* 53 (1963) 793–799.

[5] N.C. Dutta, H. Ode, Seismic reflections from a gas–water contact, *Geophysics* 48 (1983) 148–162.

[6] O.M. Lovera, Boundary conditions for a fluid-saturated porous solid, *Geophysics* 52 (1987) 174–178.

[7] V. de la Cruz, T.J.T. Spanos, Seismic boundary conditions for porous media, *Journal of Geophysics Research* 94 (1989) 3025–3029.

[8] B. Gurevich, M. Schoenberg, Interface conditions for Biot's of poroelasticity, *Journal of the Acoustical Society of America* 105 (1999) 2585–2589.

[9] A.I.M. Denneman, G.G. Drijkoningen, D.M.J. Smeulders, K. Wapenar, Reflection and transmission of waves at a fluid/porous medium interface, *Geophysics* 67 (2002) 282–291.

[10] J.F. Allard, P. Bourdier, C. Depollier, Biot waves in layered media, *Journal of Applied Physics* 60 (1986) 1926–1929.

[11] J.F. Allard, R. Rebillard, C. Depollier, W. Lauriks, A. Cops, Inhomogeneous Biot waves in layered media, *Journal of Applied Physics* 66 (1989) 2278–2284.

[12] D.P. Schmitt, Acoustic multipole logging transversely isotropic poroelastic formations, *Journal of the Acoustical Society of America* 86 (1989) 2398–2421.

[13] W. Lauriks, J.F. Allard, C. Depollier, A. Cops, Inhomogeneous waves in layered materials including fluid, solid and porous layers, *Wave Motion* 13 (1991) 329–336.

[14] A.K. Vashisth, P. Khurana, Waves in stratified anisotropic poroelastic media: a transfer matrix approach, *Journal of Sound and Vibration* 277 (2004) 239–275.
[15] M.D. Sharma, T.N. Saini, Pore alignment between two dissimilar saturated poroelastic media: reflection and refraction at the interface, *International Journal of Solids and Structures* 29 (1992) 1361–1377.
[16] S.R. Pride, A.F. Gangi, F.D. Morgan, Deriving the equations of motion for porous isotropic media, *Journal of the Acoustical Society of America* 92 (1992) 3278–3290.
[17] A.M. Kaynia, P.K. Banerjee, Fundamental solutions of Biot's equations of dynamic poroelasticity, *International Journal of Engineering Science* 31 (1993) 817–830.
[18] J. Chen, Time domain fundamental solution to Biot's complete equations of dynamic poroelasticity, part I: two-dimensional solution, *International Journal of Solids and Structures* 31 (1994) 1447–1490.
[19] M.D. Sharma, Three-dimensional wave propagation in a general anisotropic poroelastic medium: phase velocity, group velocity and polarization, *Geophysical Journal International* 156 (2004) 329–344.
[20] M.D. Sharma, 3-D wave propagation in a general anisotropic poroelastic medium: reflection and refraction at an interface with fluid, *Geophysical Journal International* 157 (2004) 947–958.
[21] M.D. Sharma, Propagation of inhomogeneous plane waves in dissipative anisotropic porous solids, *Geophysical Journal International* 163 (2005) 981–990.
[22] M.J.P. Musgrave, *Crystal Acoustics*, Holden-Day, San Francisco, 1970.
[23] B. Paulsson, J. Meredith, Z. Wang, J. Fairborn, The steepbank crosswell seismic project: reservoir definition and evaluation of steamflood technology in Alberta tar sands, *The Leading Edge* (1994) 737–747.
[24] A.K. Vashisth, M.D. Sharma, M.L. Gogna, Reflection and transmission of elastic waves at a loosely bonded interface between an elastic solid and liquid-saturated porous solid, *Geophysical Journal International* 105 (1991) 601–617.
[25] C.H. Yew, P.N. Jogi, Study of wave motions in fluid-saturated porous rocks, *Journal of the Acoustical Society of America* 60 (1979) 2–8.